Striped-type superstructure in γ-brass alloys

Y. Koyama,* J. Yoshida, H. Hoshiya, and Y. Nakamura
Department of Metallurgy, Tokyo Institute of Technology, 2-12-1 Oh-okayama, Meguro-ku, Tokyo 152, Japan
(Received 20 March 1989)

The striped-type superstructure in the γ-brass phase has been investigated both experimentally and theoretically. Electron microscopy observation shows that, in addition to the existence of the striped pattern of the striped-type superstructure, the so-called jellyfish pattern consists of three inversion domains belonging to one of two types. The analysis of the electron-diffraction pattern further leads to an important conclusion that the striped-type superstructure can be interpreted as a structure of the normal γ-brass type modulated by two incommensurate waves. On the basis of the experimental results, the electronic origin and the discommensurate structure of the striped-type superstructure are discussed. First, the relation between the Fermi surface and the repeated Brillouin zone indicates that the two incommensurate waves have wave vectors determined as a spanning vector of the flat portion of the Fermi surface. Secondly, the Ginzburg-Landau-type model, whose order parameter is the charge density due to the charge density waves, is proposed, and reproduces the experimentally obtained change in the period of the striped-type superstructure. It is also shown that there is a phase slip of $2\pi/3$ across the discommensuration. These features derived based on the model are entirely consistent with those observed experimentally. Accordingly, it is concluded that the striped-type superstructure in the γ-brass phase can be interpreted as the charge-density-wave state in the three-dimensional system.

I. INTRODUCTION

The γ-brass phase with electron-atom ratio of 21:13 is one of the so-called Hume-Rothery phases. Its structure is a complicated one having 52 atoms in a unit cell which basically consists of $3\times3\times3$ bcc unit cells (Fig. 1). Note that two atomic vacancies are involved in a unit cell and the structure loses its centrosymmetry as a result of atomic displacements around each vacancy.

Two types of long-period superstructures in the γ-brass phase, a triangular type and a striped type, have been reported so far.[1] In Cu-Al alloys, for instance, the former is found in alloys containing 35 at. % Al and the latter in alloys containing 36–38 at. % Al.[2] These superstructures are understood to be characterized by the regular array of inversion antiphase boundaries (IAB's). The IAB is described both as an inversion boundary between domains of opposite orientations of the γ-brass structure with no centrosymmetry and as an antiphase boundary with regard to the array of atomic vacancies in the unit cell.[3]

It is found that the period of the striped-type superstructure is determined by the size of the Fermi surface.[4] This seems to indicate that the superstructure is due to the appearance of charge-density waves (CDW's), that is, Fermi-surface nesting, although the CDW state in the three-dimensional system has not been generally accepted. This fact obviously leads to an incommensurate period of the superstructure. According to McMillan,[5] the energy of the incommensurate CDW is lowered when it is in phase with the lattice and then the CDW near the lock-in transition is distorted. In order to distort the CDW, waves produced from higher-order harmonics through the *umklapp* process effectively modulate a phase of the first-order CDW. The phase modulation eventually results in the discommensuration as a phase-slip region between the in-phase regions. The discommensuration has been observed in low-dimensional materials such as $2H$-$TaSe_2$ (Refs. 6–9) and $NbTe_4$,[10] and Ag-Mg alloys having the long-period superlattice.[11] Because of this, it should then be expected in the γ-brass alloys with the striped-type superstructure. From the motivations described above, we have examined features of the striped-type superstructure in Cu-Al alloys by means of electron microscopy and theoretically studied them in terms of the Ginzburg-Landau-type model of CDW formation in the superstructure.

In this paper, we report features of the striped-type superstructure in Cu–34.8 at. % Al alloys and clarify the

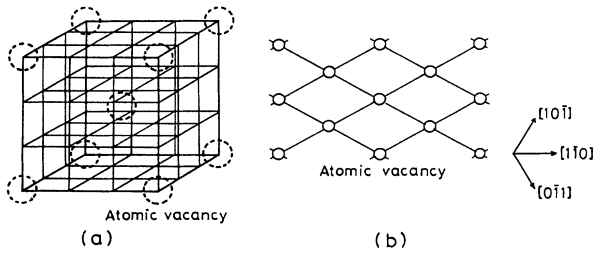

FIG. 1. Schematic diagram (a) showing features of the unit cell of the γ-brass structure and the projection (b) of the vacancy sites along the $\langle 111 \rangle$ directions. The unit cell, which basically consists of $3\times3\times3$ bcc unit cells, has two vacancies; one at the center and the other at the corner. Positions of atoms are not shown in both diagrams in order to avoid the confusion.

details of the superstructure in the viewpoint of the modulated structure. The reason why the Cu–34.8 at. % Al alloys are adopted here is that they exhibit typical features of the superstructure in the γ-brass alloys. Then, based on the experimental results, we first discuss the electronic origin of the striped-type superstructure using the concept of the Fermi-surface nesting. Further, the temperature dependence of the period of the striped-type superstructure and its discommensurate structure are discussed by means of the model Ginzburg-Landau free energy with CDW's as an order parameter.

II. EXPERIMENTAL PROCEDURES

Ingots of Cu-Al alloys containing 31–38 at. % Al were made by melting together Cu and Al at 1400 K for 12 h in vacuum and then quenched in ice water. Disk-shape specimens 12.00 mm in diameter and 0.6 mm thick cut from the ingots were annealed at 773, 873, and 973 K for 100 h in order to obtain the long-period superstructure. After they were annealed, the specimens were quenched in ice water again. The observation was carried out at room temperature using a JEM-200CX electron microscope. Specimens for the observation were prepared by electropolishing disk-shape specimens in a solution of 10% HNO_3 in methanole.

III. ELECTRON MICROSCOPY OBSERVATION OF THE STRIPED-TYPE SUPERSTRUCTURE

In the Cu–34.8 at. % Al alloys, it has been experimentally found that the striped-type superstructure exists in the alloys annealed at 773 and 873 K, and the triangular-type superstructure at 873 and 973 K. That is, when the temperature is raised, the alloy undergoes a transition from the former superstructure to the latter around 873 K. Of these two superstructures, we shall describe the features of the striped-type superstructure in this alloy below.

A bright-field image and a corresponding electron-diffraction pattern of the Cu–34.8 at. % Al alloy annealed at 773 K are shown in Fig. 2. An electron incidence is parallel to the $[\bar{1}\,\bar{1}\,\bar{1}]$ direction. The striped pattern is clearly observed as the regular array of white lines along the $[1\bar{1}0]$ direction in the image. The spacing of the lines λ is found to be about 17 nm which corresponds to a period of $n=30$, where the period of the striped-type superstructure is calculated using $n=\lambda/d_{3\bar{3}0}$ on the basis of the definition made by Morton.[4] It should be noticed that the stripe in the striped pattern is sometimes observed as black contrast, depending on the diffraction condition. In the diffraction pattern, because of the existence of the striped-type superstructure, each spot is split along the $[1\bar{1}0]$ direction. An important feature is that the split spots around the $\frac{1}{3}$ position, $h0\bar{h}$ and $0\bar{h}h$, have asymmetric intensities where h is not equal to $3n$ (h,n, integers). A careful analysis shows that a location of each spot can be consistently interpreted as that expected from a modulated structure of the γ-brass structure by means of two modulated waves. These two waves

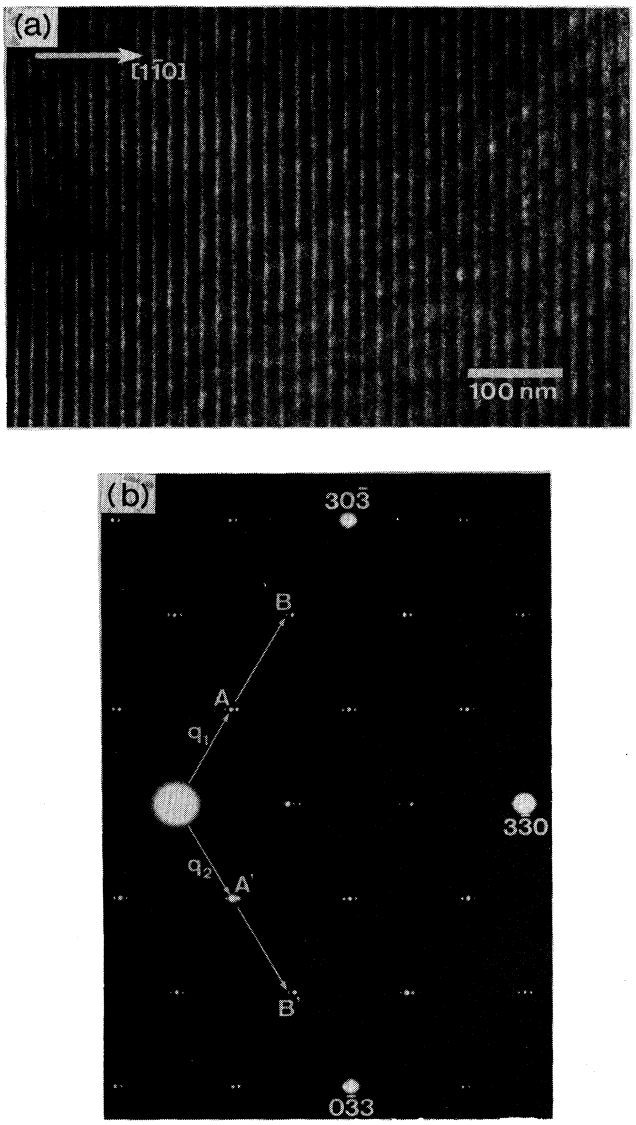

FIG. 2. Bright-field image (a) and a corresponding electron diffraction (b) of the striped-type superstructure in the Cu–34.8 at. % Al alloy annealed at 773 K for 100 h.

have incommensurate wave vectors of $\mathbf{q}_1=(1+\delta,-\delta,-1)$ and $\mathbf{q}_2=(\delta,-1-\delta,1)$ indicated in Fig. 2(b). A value of δ represents a deviation of the first-order spot from the $\frac{1}{3}$ position which is between 000 and $30\bar{3}$ for $\mathbf{q}_1$ and between 000 and $0\bar{3}3$ for $\mathbf{q}_2$. In addition, spots B and B' in the pattern are identified to be second-order harmonics of $\mathbf{q}_1$ and $\mathbf{q}_2$, respectively. Fourth- and fifth-order harmonics are also detected around the first-order spot. It should be noticed that the spacing of the stripes in the image coincides with the inverse of a distance between two neighboring spots around the $\frac{1}{3}$ position.

A characteristic pattern was found in the striped-type superstructure of the γ-brass Cu-Al alloys. Figure 3 is a bright-field image showing it, obtained from the alloy annealed at 773 K. The striped-type superstructures with

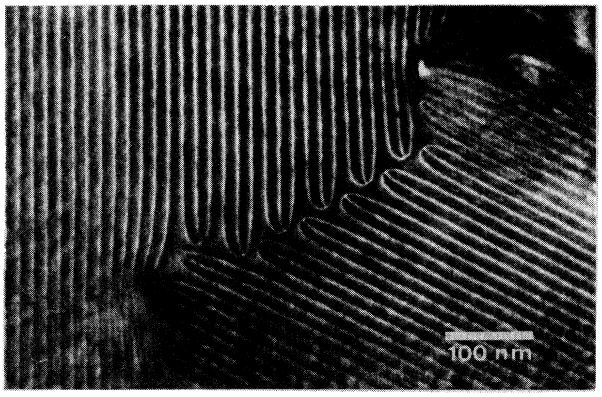

FIG. 3. Bright-field image showing the jellyfish pattern which is a characteristic pattern in the striped-type superstructure.

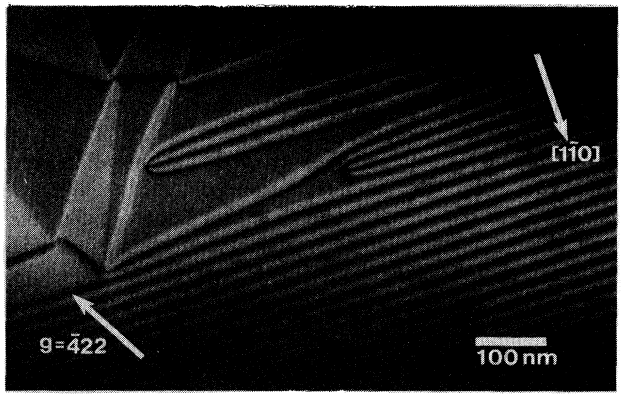

FIG. 4. Dark-field image of the Cu–34.8 at. % Al alloy annealed at 873 K. The image was actually taken under n-beam condition. The diffraction vector is $\bar{4}22$.

different modulated directions are found in the image. The characteristic pattern is observed in a boundary between these two areas having the stripes along the different directions and consists of three white lines which terminate at one point. When the regular array of the white lines is regarded as a lattice, the characteristic pattern can be said as a defect in this lattice like a dislocation in a crystal lattice. It is worth noting that the similar patterns have been already observed in $2H$-$TaSe_2$, $NbTe_4$, and Ag-Mg alloys with the long-period superlattice. In our previous paper,[11] we call these patterns a jellyfish pattern from their appearance. As is well known, this pattern is called the stripple[6] (or a CDW dislocation[5]) in $2H$-$TaSe_2$.

The bright-field images of Figs. 2(a) and 3 do not show a contrast of the inversion domain. Because the γ-brass structure does not have centrosymmetry, the violation of the Friedel's law is utilized in order to see the inversion domains.[12] Figure 4 is a dark-field image of the Cu–34.8 at. % Al alloy annealed at 873 K. An electron incidence is somewhat tilted from the $[\bar{1}\,\bar{1}\,\bar{1}]$ direction so as to violate the Friedel's law. The image was actually taken by using $\bar{4}22$ spot. In addition to the striped-type superstructure, triangular domains in the triangular-type superstructure are seen at this temperature. In the triangular-type superstructure, one of the two domains of opposite orientations of the γ-brass structure is observed as black contrast and the other as white contrast. Hence, a white ribbon represents one domain and a black ribbon the other in the striped-type superstructure. The IAB is then a boundary between the white and black ribbons. The most important thing here is that one jellyfish pattern consists of three inversion domains observed as the white ribbon; that is, the six IAB's. A relation between the inversion domain (or the IAB) and the white line in the bright-field image will be discussed later. Moreover, the period at 873 K is determined to be $n=42$ which is much larger than the period at 773 K. Note that the decrease in the period with decreasing the annealing temperature is a common feature in the striped-type superstructure of the γ-brass Cu-Al alloys. The periods at 773, 873, and 973 K for three Cu-Al alloys examined in the present experiment are listed in Table I. It is worth noting that the inverse of the distance between two neighboring spots around the $\frac{1}{3}$ position, corresponding to the period n, is twice the spacing of the regular array of the IAB's.

IV. THEORETICAL ASPECT OF THE STRIPED-TYPE SUPERSTRUCTURE

A. Electronic origin of the striped-type superstructure

Morton has already discussed a relation between the period of the striped-type superstructure and the Fermi surface in terms of the Sato-Toth theory concerning the long-period superlattice in alloys.[4] His discussion is based on the extended Brillouin zone (BZ) in Jones's fashion,[13] and then the Fermi surface determines the position of the third-order spots of $\mathbf{q}_1$ and $\mathbf{q}_2$ near the fundamental spot of the bcc structure. Because the superstructure is characterized by the periodic array of the IAB's in the γ-brass structure, however, the BZ of the γ-brass structure should be used in the construction of the BZ and the Fermi surface. Figure 5 depicts the BZ of the γ-brass structure in the case of $e/a > 21/13$. Since the Fer-

TABLE I. Experimentally obtained period n of the striped-type superstructure as a function of the annealing temperature for the Cu–34.8 at. % Al, Cu–35.0 at. % Al, and Cu–36.0 at. % Al alloys. These alloys were actually annealed at 773, 873, and 973 K. Only the triangular-type superstructure was found in both alloys containing 34.8 at. % Al and 35.0 at. % Al, annealed at 973 K.

	34.8 at. %	35.0 at. %	36.0 at. %
973 K			24
873 K	42	29	22
773 K	30	25	21

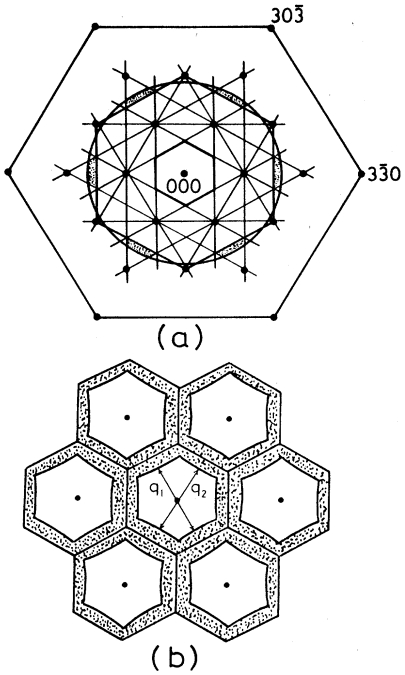

FIG. 5. Extended Brillouin zone (a) and the repeated zone (b) of the γ-brass structure, together with the Fermi surface with $e/a > \frac{21}{13}$. Dotted areas in the extended zone is reduced in the first BZ and is then repeated. In the repeated zone, the Fermi-surface nesting with wave vectors of $\mathbf{q}_1$ and $\mathbf{q}_2$ is expected along the $\langle 110 \rangle$ directions.

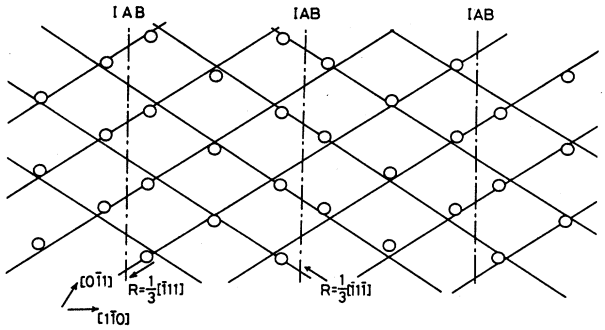

FIG. 6. Schematic diagram showing the relationship between the vacancy sites and the CDW's with incommensurate wave vectors. The diagram is the projection of the vacancy sites along the $[\bar{1}\,\bar{1}\,\bar{1}]$ direction. The solid line represents the minimum position of the negative charge due to the CDW. The actual minimum exists at a crossing point of two solid lines. An atomic vacancy occupies the nearest lattice point to the minimum. The IAB's indicated in the figure appear as a result of the production of the array of the vacancy sites with the incommensurate period.

mi surface has a flat portion along the $\langle 110 \rangle$ directions, the Fermi-surface nesting is expected along these directions. Determined nesting vectors indicated in the figure are actually understood to be the wave vectors of $\mathbf{q}_1$ and $\mathbf{q}_2$ for the modulated waves. This implies that the striped-type superstructure is the modulated structure of the normal γ-brass structure by means of CDW's with the nesting vectors of $\mathbf{q}_1$ and $\mathbf{q}_2$. It is obvious that this interpretation is identical to that obtained from the analysis of the diffraction pattern. From Fig. 5(b), the relation between the period n and the electron-atom ratio is expressed as

$$\frac{e}{a}=\frac{\sqrt{2}\pi}{78t^3}\left[4-\left[1\pm\frac{1}{n}+\frac{1}{n^2}\right]^{1/2}\right]^3, \tag{1}$$

where t is a truncation factor which represents the deviation of the Fermi sphere, and the positive sign is used for $e/a \leq 21/13$ and the negative one for $e/a > 21/13$. Based on Eq. (1), the change in the period against the electron-atom ratio was calculated. In addition to the Cu-Al alloys, the calculated change was found to be basically consistent with the observed ones in Ni-Zn, Cu-Zn, and Pd-Zn alloys, which has been reported,[14] although a factor to be described later should be taken into account. Furthermore, the positional correspondence between the sites of the atomic vacancies and the CDW's shows that the CDW's determine the arrangement of the atomic vacancies involved in the unit cell, as shown in Fig. 6. This implies that in the striped-type superstructure the charge produced from the appearance of the CDW's is mainly compensated by the rearrangement of the atomic vacancies instead of the periodic lattice distortion (PLD) in the low-dimensional materials such as $2H$-$TaSe_2$.[15] Note that the vacancies are originally arranged along the $\langle 110 \rangle$ directions in the normal γ-brass structure, as shown in Fig. 1(b).

B. Ginzburg-Landau theory for the striped-type superstructure

The present experiment shows that the period of the striped-type superstructure has the temperature dependence as well as the compositional dependence. In the γ-brass Cu-Al alloys, the period n decreases with decreasing temperature, for instance, $n=42$ at 873 K and $n=30$ at 773 K in the Cu–34.8 at. % Al alloys. This implies that the nesting vectors of $\mathbf{q}_1$ and $\mathbf{q}_2$ obtained experimentally deviate from those determined originally by the size of the Fermi surface. The deviation is obviously a result of an effort of the alloy in order that the energy of the incommensurate CDW is lowered. Such an effort has been actually found in $2H$-$TaSe_2$. Based on a similar Ginzburg-Landau theory to that proposed by McMillan for $2H$-$TaSe_2$,[5] we discuss the temperature dependence of the period of the striped-type superstructure and the discommensurate structure in the γ-brass alloys.

It is understood on the basis of the present experimental results that in the striped-type superstructure the normal phase has the γ-brass structure without any IAB's and the modulated waves are those with the nesting vectors of $\mathbf{q}_1$ and $\mathbf{q}_2$. It is therefore reasonable to assume that the striped-type superstructure appears as a result of the transition from the normal γ-brass phase although the triangular-type superstructure exists between them. The transition is due to the appearance of the CDW's.

The electronic charge density of the striped-type superstructure is hence written as

$$\rho(\mathbf{r})=\rho_0(\mathbf{r})[1+\eta(\mathbf{r})] , \tag{2}$$

where $\eta(\mathbf{r})$ is the real order parameter related to the appearance of the CDW's and $\rho_0(\mathbf{r})$ is the charge density of the normal γ-brass structure. The complex order parameter Φ is related to the real order parameter by $\eta(\mathbf{r})=\mathrm{Re}(\Phi)$, where Φ includes the contribution from the higher-order harmonics. In the case that the striped-type superstructure exists along the $[1\bar{1}0]$ direction, as shown in Fig. 2, the complex order parameter for the first-order CDW's can be, at first, expressed as

$$\Psi_0=\psi_{00}\exp(i\mathbf{q}_1\cdot\mathbf{r})+\psi_{00}\exp(i\mathbf{q}_2\cdot\mathbf{r}) \tag{3}$$

using the waves with the nesting vectors,

$$\begin{aligned}\mathbf{q}_1&=\tfrac{1}{3}\mathbf{G}_{30\bar{3}}+\tfrac{1}{3}\delta\mathbf{G}_{3\bar{3}0} ,\\ \mathbf{q}_2&=\tfrac{1}{3}\mathbf{G}_{0\bar{3}3}+\tfrac{1}{3}\delta\mathbf{G}_{3\bar{3}0} ,\end{aligned} \tag{4}$$

where $\mathbf{G}$ is a reciprocal-lattice vector of the normal γ-brass structure. From the definition made by Morton,[4] the period of the striped-type superstructure is calculated as $n=1/\delta$. As described above, the vectors $\mathbf{q}_1$ and $\mathbf{q}_2$ do not coincide with those determined by the size of the Fermi surface. After some algebraic manipulations, we obtain

$$\Psi_0=\bar{\psi}_{00}\exp[i(\tfrac{1}{6}+\tfrac{1}{3}\delta)\mathbf{G}_{3\bar{3}0}\cdot\mathbf{r}] , \tag{5}$$

where

$$\bar{\psi}_{00}=2\psi_{00}\cos(\tfrac{1}{2}\mathbf{G}_{\bar{1}\bar{1}2}\cdot\mathbf{r}) . \tag{6}$$

Note that $\bar{\psi}_{00}$ includes only the periodicity along the $[\bar{1}\,\bar{1}2]$ direction perpendicular to the $[1\bar{1}0]$ direction; that is, a direction of the superstructure, and the period coincides with that of the normal γ-brass structure. Because of this, we neglect the position dependence of $\bar{\psi}_{00}$ for convenience sake. Hence, we can deal with the striped-type superstructure in terms of the one-dimensional modulated structure which is characterized by the modulated wave given by Eq. (5). Further, when the higher-order harmonics observed in the diffraction pattern of Fig. 1(b) are taken into account, the complex order parameter eventually becomes

$$\Phi=\sum_j\Psi_j=\sum_j\bar{\psi}_{j0}\exp(iQ_j\mathbf{G}_{3\bar{3}0}\cdot\mathbf{r}) , \tag{7}$$

where $Q_j=\frac{1}{6}+(j+\frac{1}{3})\delta$. Values for j, corresponding to the first-, second-, fourth-, and fifth-order waves, are 0, -1, 1, and -2, respectively.

The similar Ginzburg-Landau free energy to that proposed by McMillan[5] for $2H$-$TaSe_2$ is used in the present calculation,

$$F=\int d\mathbf{r}\,[K|(\nabla-i\bar{Q}_0\mathbf{G}_{3\bar{3}0})\Phi|^2+a\eta^2+b\eta^3+c\eta^4] , \tag{8}$$

where $\bar{Q}_0$ is calculated from δ_0 $(=1/n_0)$ which is determined by the size of the Fermi surface. Since the free energy is invariant with respect to the translation symmetry of the normal γ-brass structure, coefficients, K, a, b, and c must have the following form, for instance,

$$b=b_0+\sum_m b_m\exp(-i\mathbf{G}_m\cdot\mathbf{r}) , \tag{9}$$

where $\mathbf{G}_m$ is a reciprocal-lattice vector of the normal γ-brass structure. The temperature dependence is assumed to be $a_0=a'(T-T_0)$, as in the conventional Landau theory. By substituting Eq. (7) into (8), the free energy becomes

$$\begin{aligned}F=&\sum_j\sum_{j'}K\bar{\psi}_{j0}\bar{\psi}^*_{j'0}(Q_j-\bar{Q}_0)(Q_{j'}-\bar{Q}_0)\mathbf{G}^2_{3\bar{3}0}\delta(Q_j-Q_{j'})+\tfrac{1}{4}\sum_j\sum_{j'}a\bar{\psi}_{j0}\bar{\psi}_{j'0}\delta(Q_j+Q_{j'})\\&+\tfrac{1}{8}\sum_j\sum_{j'}\sum_{j''}b\bar{\psi}_{j0}\bar{\psi}_{j'0}\bar{\psi}_{j''0}\delta(Q_j+Q_{j'}+Q_{j''})+\tfrac{1}{16}\sum_j\sum_{j'}\sum_{j''}\sum_{j'''}c\bar{\psi}_{j0}\bar{\psi}_{j'0}\bar{\psi}_{j''0}\bar{\psi}_{j'''0}\delta(Q_j+Q_{j'}+Q_{j''}+Q_{j'''}) ,\end{aligned} \tag{10}$$

where $\delta(Q_j)=1$ for $Q_j=0$ or for $Q_j=G_m/G_{3\bar{3}0}$, and $\delta(Q_j)=0$ otherwise. The coefficients in the free-energy expression are determined in the following rule, for instance,

$$b=\begin{cases}b_0: & Q_j+Q_{j'}+Q_{j''}=0,\\ b_m: & Q_j+Q_{j'}+Q_{j''}=G_m/G_{3\bar{3}0}.\end{cases} \tag{11}$$

In the present work, we assume that for simplicity $\bar{\psi}_{j0}$ is a real parameter (ϕ_j) and mainly use a free energy for four waves; that is, the first-, second-, fourth-, and fifth-order waves, which are observed in the electron-diffraction pattern. Values of ϕ_j and δ $(=1/n)$ at each temperature are determined so as to minimize the free energy.

In order to determine the discommensurate structure, the phase and amplitude modulations are obtained in the following way. From Eq. (7), the order parameter is written as

$$\Phi=A\exp[i(\tfrac{1}{6}\mathbf{G}_{3\bar{3}0}\cdot\mathbf{r}+\theta)] , \tag{12}$$

where A and θ are, respectively, an amplitude and a phase of the resultant complex order parameter. When α and β are assumed to be

$$\begin{aligned}\alpha&=\sum_j\phi_j\cos[(j+\tfrac{1}{3})\delta\mathbf{G}_{3\bar{3}0}\cdot\mathbf{r}] ,\\ \beta&=\sum_j\phi_j\sin[(j+\tfrac{1}{3})\delta\mathbf{G}_{3\bar{3}0}\cdot\mathbf{r}] ,\end{aligned} \tag{13}$$

A and θ can be expressed in the simple forms of

$$\begin{aligned}A&=(\alpha^2+\beta^2)^{1/2} ,\\ \theta&=\tan^{-1}(\alpha/\beta) .\end{aligned} \tag{14}$$

Both modulations can be hence calculated from ϕ_j determined by minimizing the free energy.

Figure 7 shows the temperature dependence of the period n for various values n_0 determined by the size of the Fermi surface. The calculation was made by using the parameters, $a'=T_0=1.0$, $b_3=2.0$, $c_0=9.5$, and $K_0G^2_{3\bar{3}0}=7.0$. The normal γ-brass structure exists above $T=1.0$. In Fig. 7, the period decreases with decreasing temperature and the degree of the change is larger with larger n_0. In $n_0=5$, in fact, the period is almost independent of temperature. In addition, although the correspondence between the reduced temperature in the calculation and the experimental one is not obvious, the curve for $n_0=20$ seems to reproduce the change in the Cu–34.8 at. % Al alloys; $n=42$ at 873 K and $n=30$ at 773 K. Accordingly, it is concluded that the features of the experimentally obtained change shown in Table I can be explained in terms of the present Ginzburg-Landau-type model. It should be noticed that the triangular-type superstructure appears between the normal phase above $T=1.0$ and the striped-type one in lower temperatures. The calculated values just below $T=1.0$ are hence omitted for all curves in Fig. 7.

The amplitude and phase modulations against the position along the $[1\bar{1}0]$ direction are shown in Fig. 8. Both were calculated for $n_0=20$ at $T=0.8$. The period in this case is $n=45.1$, which is almost the same as that at 873 K in the Cu–34.8 at. % Al alloy. Normalized real parameters with respect to the first-order wave ϕ_0, which were actually used in the calculation, are $\phi_{-1}:\phi_1:\phi_{-2}=0.368:-0.072:-0.042$ and are compatible with the intensities of the spots in the diffraction pattern of Fig. 1(b). In Fig. 8, the phase versus position curve consists of a region with a constant-phase and a phase-slip region between them. Based on Eq. (12), the constant-phase region is understood to be an in-phase region and the phase-slip region a discommensuration. In addition, there is the phase slip of $2\pi/3$ across one discommensuration. The distance between two neighboring discommensurations is found to be $1/\delta=n$. This clearly implies that the period n does not characterize the regular array of the IAB's, but that of the discommensurations. Because of $(2\pi/3)\times 3=2\pi$, a jellyfish pattern is also expected to consist of three discommensurations, just as in $2H$-$TaSe_2$. As for the amplitude modulation, the modulation is almost sinsoidal and its minimum appears at the discommensuration.

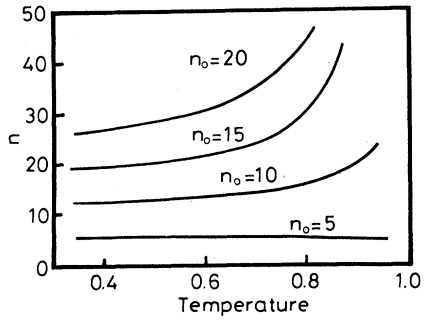

FIG. 7. Calculated period n of the striped-type superstructure against temperature. The period is defined as $n=\lambda/d_{3\bar{3}0}$ and the temperature is normalized with respect to T_0, so that both are dimensionless parameters.

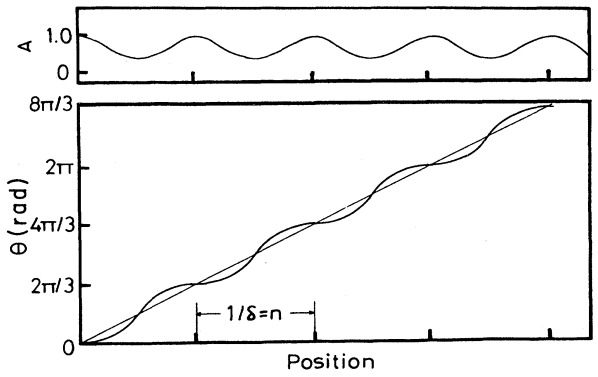

FIG. 8. Amplitude and phase modulations of the first-order CDW at $T=0.8$ for $n_0=20$. The calculation was made using the same parameters as those for the period shown in Fig. 7. The position and the amplitude A are, respectively, normalized with respect to $d_{3\bar{3}0}$ and the maximum value of A, and then are dimensionless parameters. In the diagram, n is equal to 45.1.

V. DISCUSSION

The present calculation based on the Ginzburg-Landau model shows that there is the phase slip of $2\pi/3$ across the discommensuration. Based on Eq. (12), the magnitude of $2\pi/3$ is determined to be equivalent to the displacement vector of $\mathbf{R}=\frac{2}{3}(-1,1,0)$. As shown in Fig. 6, on the other hand, the IAB is divided into two types, A type and B type, on the basis of the displacement vectors associated with the array of the atomic vacancies. When the A-type IAB has the vector of $\mathbf{R}_1=\frac{1}{3}(-1,1,1)$, the B-type one has $\mathbf{R}_2=\frac{1}{3}(-1,1,-1)$. Actually, these displacement vectors have been recently confirmed by high-resolution electron microscopy observation.[3] The most important thing to understand the relation between the discommensuration and the IAB is that there exists the relation among the vectors: $\mathbf{R}=\mathbf{R}_1+\mathbf{R}_2$. That is, the sum of these vectors leads to the phase slip of $2\pi/3$. Because the inversion domain is sandwiched by one A-type IAB and one B-type IAB, there is the phase slip of $2\pi/3$ across one inversion domain. In other words, one of two domains of opposite orientations is concluded to serve as the discommensuration to the other. The jellyfish pattern as the defect in the discommensuration lattice is further expected to consist of three inversion domains which give rise to the same contrast in the dark field image. In Fig. 4, the jellyfish pattern is in fact observed as the combination of three white ribbons. Accordingly, there is no inconsistency between the experimental results and the Ginzburg-Landau model. It should be remarked that the discommensurate structure in the striped-type superstructure of the γ-brass alloy is very similar to that in the

striped phase of $2H$-$TaSe_2$, which is obtained by heating from the commensurate phase.[6,7] Moreover, it can be pointed out on the basis of the above discussion that it is possible to regard these two types of the IAB's as dissociated antiphase boundaries proposed by Snykers, Delavignette, and Amelinckx.[16] They have not, however, discussed a physical origin of the appearance of the dissociated antiphase boundary. In other words, the physical relation between the dissociated antiphase boundary and the discommensuration remains unsolved. In spite of this, we believe that it is presumably important to point out the similarity between their crystallographic features.

In the bright-field image of Fig. 3, the jellyfish pattern is observed as the combination of three white lines. As mentioned just above, two types of the IAB's with the different displacement vectors, R_1 and R_2, exist in the superstructure. Because of this, only the IAB's with the same type of the vectors can be observed in a bright-field image on the basis of the usual extinction rule. Among the six IAB's forming the jellyfish pattern, then the pattern is observed as the combination of three IAB's with the same vector; that is, three white lines in Fig. 3. It is further understood that the spacing of the white lines in Figs. 2(a) and 3 coincides with that of the discommensurations. This implies that the array of the white lines simply reflects that of the discommensurations rather than that of the IAB's. In other words, the regular array of the discommensurations is characterized by the period n defined by Morton.

In addition to the first-, second-, fourth- and fifth-order spots around $\frac{1}{3}$ position, the third-order one near the fundamental spot of the bcc structure is also observed in the diffraction pattern. Morton used the third-order spot in his discussion on the relationship between the period n and the Fermi surface. This spot never, however, has a stronger intensity than the first-order spot and then cannot be regarded as a major modulated wave. In addition, the BZ of the γ-brass structure should be adopted in his discussion, as described earlier. It is therefore obvious that his discussion is inappropriate. The reasons why his discussion can work are that the third-order spot is located at a position determined by the size of the Fermi surface in the Jones's fashion and the distance between the third-order spot and the fundamental spot of the bcc structure is δ which is, of course, equal to $1/n$. Hence, it is worth remarking that the period n, in fact, characterizes the array of the discommensurations. In our treatment, the Fermi surface determines the position of the first-order spot and then the third-order spot (harmonic) plays a role in making a square modulation.

A lock-in transition to a commensurate structure was not found in the striped-type superstructure. In the superstructure, the location of the first-order spot is very close to that of the fundamental spot of the normal γ-brass structure; that is, the $\frac{1}{3}$ position. Because of this, there is no stable commensurate structure like the commensurate $M=2$ structure in the long-period superlattice in alloys.[5] Accordingly, no commensurate structure is basically expected in lower temperatures in the striped-type superstructure.

As found in the present experiment, the period n decreases with decreasing temperature. This change corresponds to an increase in the number of the IAB's in a unit distance and then is in contrast to the change found in $2H$-$TaSe_2$. According to our calculation, the discommensurate structure is sufficiently developed in relatively higher temperatures for large n_0, as shown in Fig. 8. Although the temperature dependence of ϕ_j is not presented here, the relative magnitude of ϕ_0 against the others is found to increase with decreasing temperature. This implies that the increase in ϕ_0 leads to the decrease in the period. It should be remarked that the lock-in transition usually occurs on cooling if a stable commensurate structure exists. From the reason described above, however,there is no stable commensurate structure in the γ-brass phase. Hence, it can be understood that the decrease in the period represents an effort of the alloy with no stable commensurate structure in order to gain the energy after developing the discommensurate structure. That is, the alloy obtains the energy gain by further opening the band gap at the Fermi surface at the expense of the developed discommensurate structure.

The stability of the triangular-type superstructure has been discussed already in terms of the Ginzburg-Landau theory by Yamada and Koh.[17] Because the period of the triangular-type superstructure has not been reported to exhibit the electron-atom ratio dependence and the features of the superstructure are analogous to those observed in quartz, they adopted the macroscopic strain as an order parameter with the bcc structure as a normal structure. Based on their theory, they could show the appearance of the triangular-type superstructure. This implies that the physical origin of the triangular-type superstructure is entirely different from that of the striped-type one. The difference in the physical origin gives us the motivation for examining the transition between these superstructures. In order to investigate the details of the transition, we will plan an experiment on it.

It is found in the present work that the features of the striped-type superstructure can be explained in the viewpoint of the CDW formation although the formation in the three-dimensional system has not been accepted. It is well understood that the formation, of course, leads to a gain in energy because of the band gap at the Fermi surface. On the other hand, the Coulomb field induced by the appearance of the CDW must be screened by the positive ion. In the case of the low-dimensional system, the screening is made by the periodic lattice distortion. In spite of the energy loss due to the PLD, the CDW can appear in the low-dimensional system owing to a large energy gain originating from the large flat portion of the Fermi surface. Generally speaking, the small flat portion in the three-dimensional system prevents the CDW formation. It should be noticed that the introduction of the antiphase boundary in the ordered structure can produce an incommensurate period for the array of the positive ions. It is obvious that the energy loss due to the introduction of the antiphase boundary is much smaller than that due to the PLD. If the screening takes place by the appearance of the antiphase boundary, the CDW state should be expected in the three-dimensional system, as has already been discussed in the long-period superlattice

in alloys.[11] We believe that this is realized in the striped-type superstructure in the γ-brass phase.

Finally, it should be remarked that similar patterns to the jellyfish pattern found in the γ-brass alloy have been already observed in χ-phase alloys,[16] Au_5Mn (Ref. 18), and Ni_3Mo (Refs. 19 and 20) by Amelinckx *et al.* They have investigated crystallographic features of these patterns in detail and then interpreted the patterns in terms of the concept of the dissociated antiphase boundary. In order to clarify whether such patterns are characterized as a defect in the discommensuration lattice resulting from the phase modulation of incommensurate CDW's, a theoretical consideration based on the Ginzburg-Landau-type model is definitely needed, just as in the present case of the γ-brass alloy and that of $2H$-$TaSe_2$. If a physical origin for the dissociated antiphase boundary is the phase modulation of the incommensurate CDW's, it is understood that the CDW state is realized in these alloys. In other words, the appearance of the CDW is not a special phenomenon, which can be expected only in the low-dimensional system, but can occur in the three-dimensional ordered alloys whose Fermi surfaces have flat portions in some directions. As mentioned above, in the ordered alloys, the Coulomb field due to the CDW's is screened by the introduction of the antiphase boundary, which results in the array of the positive ions with an incommensurate period.

In conclusion, the experimentally obtained features of the striped-type superstructure can be well explained in terms of the present Ginzburg-Landau-type model, in which the order parameter is assumed to be the electronic charge density due to the CDW's. It can be concluded that the striped-type superstructure of the γ-brass alloy is characterized by the appearance of the CDW's in the three-dimensional system.

APPENDIX

1. Q_j for the higher-order spots

In the electron diffraction pattern of Fig. 2(b), the higher-order spots are observed around the $\frac{1}{3}$ position; that is, the position of the diffraction spot of the normal γ-brass structure. Locations of the higher-order spots are schematically depicted in Fig. 9. As shown in Fig. 9, the first-order spot is $\frac{1}{3}\delta\mathbf{G}_{3\bar{3}0}$ apart from the $\frac{1}{3}$ position, so that the second-order one appears at $-\frac{2}{3}\delta\mathbf{G}_{3\bar{3}0}$ from it. The spots are then arranged in a spacing of $\delta G_{3\bar{3}0}$. Accordingly, Q_j is given by

$$Q_j=\tfrac{1}{6}+(j+\tfrac{1}{3})\delta\ , \tag{A1}$$

where the first-, second-, fourth-, and fifth-order spots have the j values of 0, -1, 1, and -2, respectively.

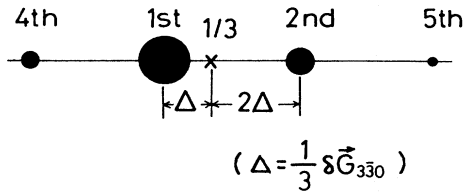

FIG. 9. Schematic representation of higher-order spots close to the $\frac{1}{3}$ position in the electron-diffraction pattern of Fig. 2(b).

2. Free-energy expression for four waves

The free energy is, in the general form, given by Eq. (10). Here, we show the expression of the free energy for four waves; that is, the first-, second-, fourth-, and fifth-order waves, derived from the equation.

Because of the nature of $\delta(Q_j-Q_{j'})$ and $\delta(Q_j+Q_{j'})$, the harmonic term in the free energy can be, at first, written as

$$\sum_{j=-2}^{1}[K_0(Q_j-\bar{Q}_0)^2G_{3\bar{3}0}^2+\tfrac{1}{2}a_0]\phi_j^2 \tag{A2}$$

using the real parameter ϕ_j. The first term in Eq. (A2) is usually called the elastic term.

In the case of the γ-brass structure, the third-order term is extremely important. This is because this term originates from the *umklapp* process; that is $(Q_j+Q_{j'}+Q_{j''})\mathbf{G}_{3\bar{3}0}=\mathbf{G}_m$. Figure 10 shows a schematic diagram which is used in order to pick up the third-order terms for four waves. With the help of the diagram, we can take

$$\tfrac{3}{8}b_3(\phi_0^2\phi_{-1}+2\phi_0\phi_{-1}\phi_{-2}+\phi_{-1}^2\phi_1)\ , \tag{A3}$$

which are called the *umklapp* term. As is well under-

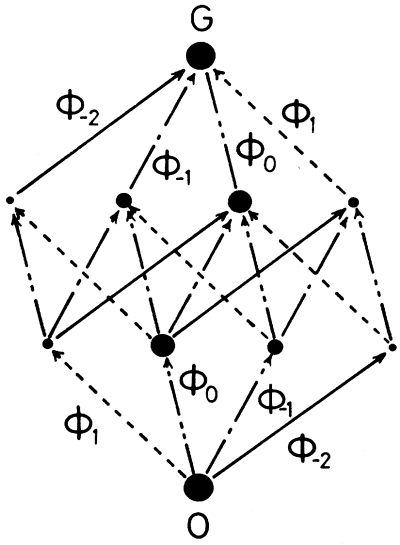

FIG. 10. Schematic diagram showing the locations of higher-order spots in the electron-diffraction pattern in order to pick up the *umklapp* term. Note that the diagram is extremely exaggerated. Large closed circles, O and G, represent the fundamental spots and ϕ_0, ϕ_{-1}, ϕ_1, and ϕ_{-2} correspond to the real parameters of the first-, second-, fourth-, and fifth-order spots, respectively.

stood in the low-dimensional system, the *umklapp* term plays an essential role in both the change in the period and the discommensurate structure.

Further, we can easily pick up the fourth-order term

$$\tfrac{3}{8}c_0(\phi_0^4+\phi_1^4+\phi_1^4+\phi_2^4)+\tfrac{3}{2}c_0(\phi_0^2\phi_{-1}^2+\phi_0^2\phi_1^2+\phi_0^2\phi_{-2}^2 +\phi_{-1}^2\phi_1^2+\phi_{-1}^2\phi_{-2}^2+\phi_1^2\phi_{-2}^2) \quad \text{(A4)}$$

because of the condition, $Q_j+Q_{j'}+Q_{j''}+Q_{j'''}=0$. By collecting the terms, (A2)+(A3)+(A4), we obtain the final expression of the free energy for the four waves. This free energy has been mainly used in the present calculation. That is, both ϕ_j and n were determined by minimizing this free energy with respect to ϕ_j and n. The calculation was actually carried out by the iteration method.

*Present address: Department of Materials Science and Engineering, Waseda University, 3-4-1 Ohkubo, Shinjuku-ku, Tokyo 169, Japan.

[1]A. J. Morton, Phys. Status Solidi A **31**, 661 (1975); **33**, 395 (1976).

[2]M. Van Sande, J. Van Landuyt, M. Avalos-Borja, G. T. Villansenor, and S. Amelinckx, Mater. Sci. Eng. **46**, 167 (1980).

[3]Y. Nakamura and H. Koike (unpublished).

[4]A. J. Morton, Phys. Status Solidi A **44**, 205 (1977).

[5]W. L. McMillan, Phys. Rev. B **12**, 1187 (1975); **14**, 1496 (1976).

[6]K. K. Fung, S. McKernan, J. W. Steed, and J. A. Wilson, J. Phys. C **14**, 5417 (1981).

[7]C. H. Chen, J. M. Gibson, and R. M. Fleming, Phys. Rev. B **26**, 184 (1982).

[8]T. Onozuka, N. Otsuka, and H. Sato, Phys. Rev. B **34**, 3303 (1986).

[9]Y. Koyama, Z. P. Zhang, and H. Sato, Phys. Rev. B **36**, 3701 (1987).

[10]J. Mahy, J. Van Landuyt, S. Amelinckx, Y. Uchida, K. D. Bronsema, and S. Van Smaalen, Phys. Rev. Lett. **55**, 1496 (1976).

[11]Y. Fujino, H. Sato, M. Hirabayashi, E. Aoyagi, and Y. Koyama, Phys. Rev. Lett. **58**, 1012 (1987).

[12]R. Serneels, M. Snykers, P. Delavignette, R. Gevers, and S. Amelinckx, Phys. Status Solidi B **58**, 277 (1973).

[13]H. Jones, *The Theory of Brillouin Zone and Electronic States in Crystals* (North-Holland, Amsterdam, 1960), pp. 207–213.

[14]A. J. Morton, in *Modulated Structure—1979 (Kailua Kona, Hawaii),* Proceedings of the International Conference on Modulated Structures AIP Conf. Proc. No. 53, edited by J. M. Cowley, J. B. Cohen, M. B. Salamon, and B. J. Wuensch (AIP, New York, 1979), pp. 241–243.

[15]S.-K. Chan and V. Heine, J. Phys. F **3**, 795 (1973).

[16]M. Snykers, P. Delavignette, and S. Amelinckx, Phys. Status Solidi B **48**, K1 (1971).

[17]Y. Yamada and S. Koh, J. Phys. F **18**, 1371 (1988).

[18]E. Ruedl and S. Amelinckx, Phys. Status Solidi A **84**, 185 (1984).

[19]G. Van Tendeloo, J. Van Landuyt, P. Delavignette, and S. Amelinckx, Phys. Status Solidi A **25**, 697 (1974).

[20]G. Van Tendeloo, P. Delavignette, R. Gevers,and S. Amelinckx, Phys. Status Solidi A **18**, 85 (1973).

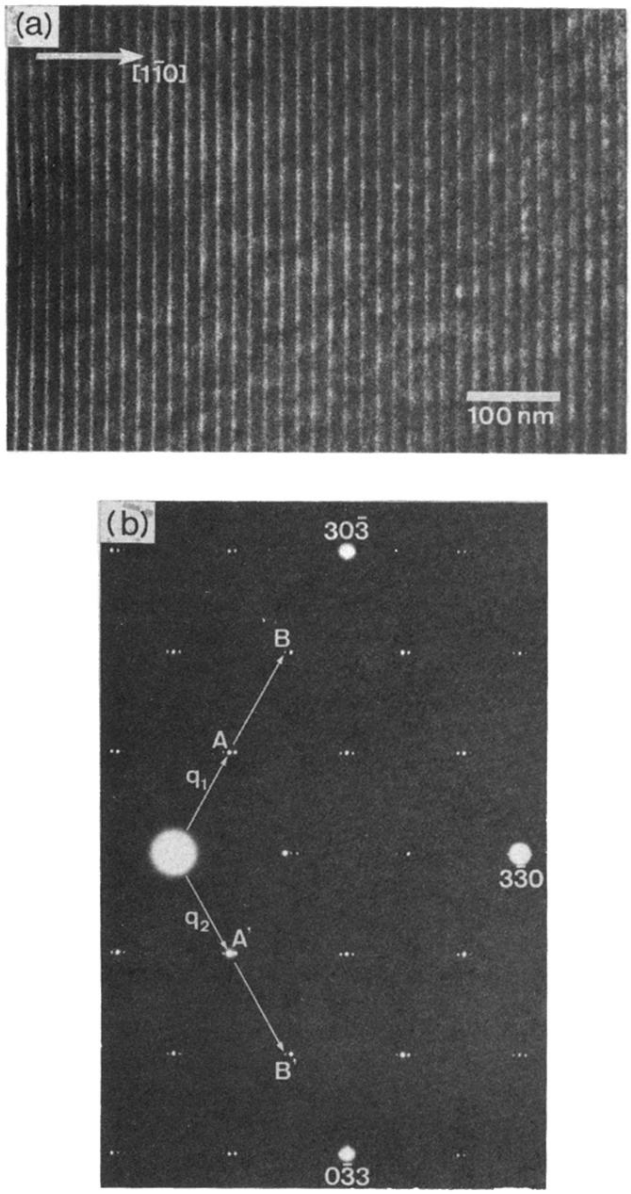

FIG. 2. Bright-field image (a) and a corresponding electron diffraction (b) of the striped-type superstructure in the Cu–34.8 at. % Al alloy annealed at 773 K for 100 h.

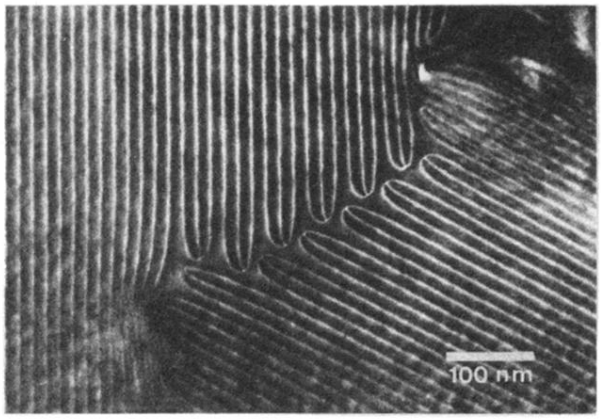

FIG. 3. Bright-field image showing the jellyfish pattern which is a characteristic pattern in the striped-type superstructure.

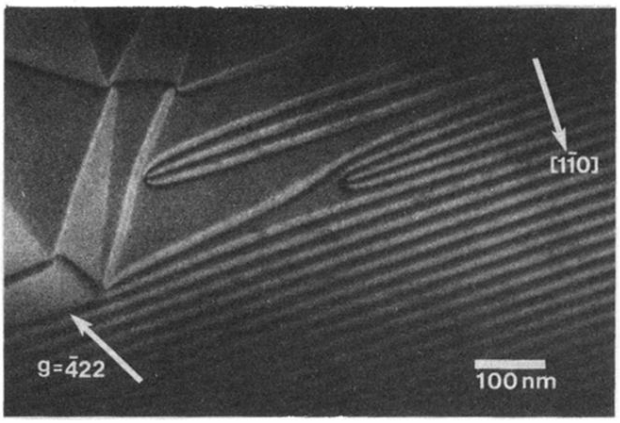

FIG. 4. Dark-field image of the Cu–34.8 at. % Al alloy annealed at 873 K. The image was actually taken under *n*-beam condition. The diffraction vector is $\bar{4}22$.